International Journal of Grid and Distributed Computing
Vol. 10, No. 1 (2017), pp.87-98
http://dx.doi.org/10.14257/ijgdc.2017.10.1.09

Multi-agent based IWD Power State Estimation of Unbalanced Grid Constraints Integrated

Li Shuqiang

College of Agricultural Engineering, Henan University of Science and Technology,
Luoyang 471003, China
E-mail: dr_lsq@163.com

Abstract

In allusion to the state estimation of the three-phase imbalance power distribution network, the multi-agent intelligent water drop optimization method with constraint integrated items is designed in this paper. Firstly, the mathematical model of the three-phase imbalance power distribution network is researched, and meanwhile the state estimation fitness function with constraints integrated items is designed according to the characteristics of the co-evolution algorithm in order to realize the unconstrained operation of the algorithm; secondly, the multi-agent co-evolution method is adopted to improve IWD (Intelligent Water Drop) algorithm, wherein each agent is responsible for optimizing a cluster, and each sub-agent is responsible for executing a one-dimensional evolution process on the basis of the evolution of the management agent, and the sub-agent evolution results are continuously introduced therein during the evolution of the management agent in order to update the dimensionality of the global optimal solution, thus to realize the collaborative balanced decomposition of the high-dimensional optimization problem. Finally, the state estimation comparison experiment carried out on IEEE 57-bus and 123-bus standard calculation instances shows that the proposed method has high estimation accuracy in the aspect of the state estimation error index, and the proposed algorithm is proven to have high calculation efficiency according to the comparison under different network scales.

Keywords: *Constraints integrated; State estimation; Power distribution network; Co-evolution; MAIWD (Multi-agent Based Intelligent Water Drop) algorithm; Three-phase imbalance; Multi-agent*

1. Introduction

The essence for solving the state estimation problem of the power distribution network is to adopt relevant computer technology and mathematical processing algorithm for the parameter fitting, prediction and correction of the measured data with redundancy and relevancy in order to improve the integrity and the reliability of the processed data, thus to obtain the accurate real-time state information of the power distribution network [1~2]. In a power distribution network, the following three conditions can disturb the flow balance of the three-phase power distribution network, namely: (1) line asymmetry; (2) access of distributed generator; (3) load imbalance, so it is necessary to estimate the state of the power distribution network to remove the three-phase imbalance. In Literature [4], the research on the state estimation of the three-phase power distribution network is mainly carried out from the angles of measurement conversion and performance improvement, but the emphasis is not attached to the three-phase balance maintenance. In Literature [5], in allusion to the slightly changed voltage phase angle, the coordinate conversion tool is adopted to make Jacobian matrix parameter become a constant; although the algorithm

ISSN: 2005-4262 IJGDC

has good real-time performance, yet it is only applicable to the three-phase power distribution network with small imbalance and light load. Therefore, the multi-agent co-evolution method is adopted in this paper to improve MAIWD algorithm (Multi-agent based IWD), wherein each agent is responsible for optimizing a cluster, and each sub-agent is responsible for executing a one-dimensional evolution process on the basis of the evolution of the management agent, and the sub-agent evolution results are continuously introduced therein during the evolution of the management agent in order to update the dimensionality of the global optimal solution, thus to realize the collaborative balanced decomposition of the high-dimensional optimization problem.

2. Unbalanced Power Grid Constraints Integration Model

2.1. Objective Function

The state estimation process of the unbalanced power grid is essential to improve the approximation degree between the measurement and the estimator. The common method is the weighted least square (WLS) method, and the optimized mathematical model can be represented as follows:

$$\min f(x) = \sum_{i=1}^{m} \omega_i \left[z_i - h_i(x) \right]^2 \tag{1}$$

In Formula (1), *zi* is the measured value of the *i*th state, *x* is the state variable, *wi* is the weight coefficient of the *i*th state, *hi(x)* is the corresponding state fitting function for the variable from the mapping state to the *i*th measurement state, and *m* is the quantity of the measurement states.

2.2. Constraints Integration

The inequality constraints existing in the three-phase power distribution network include: the active and reactive constraints of the load, the current circuit constraint, the active constraint of the distributed generator and the voltage node constraint. The mathematical inequality description is as follows:

$$\begin{cases} P^i_{\mathrm{LD,min}} \le P^i_{\mathrm{LD}} \le P^i_{\mathrm{LD,max}} \\ Q^i_{\mathrm{LD,min}} \le Q^i_{\mathrm{LD}} \le Q^i_{\mathrm{LD,max}} \\ P^i_{\mathrm{DG,min}} \le P^i_{\mathrm{DG}} \le P^i_{\mathrm{DG,max}} \\ I^{ij}_{\mathrm{LN}} \le I^{ij}_{\mathrm{LN,max}} \\ V^i_{\mathrm{ND,min}} \le V^i_{\mathrm{ND}} \le V^i_{\mathrm{ND,max}} \end{cases} \tag{2}$$

Where the variable subscript refers to the distributed generator, LD represents the load, ND represents the node, LN represents the circuit, *i* and *j* are the state identifications of the measured object.

The equality constraints, also called as flow constraint, are formally represented as follows according to relevant calculation formulae of the flow algorithm for node, branch current and node voltage.

$$\begin{cases} I^i = \left(S^i / V^i \right)^* \\ I^{ij} = -I^j + \sum_{k \in C} I^{jk} \\ V^j = V^i - Z^{ij} I^{ij} \end{cases} \tag{3}$$

Where *Ii* represents the injected node current, *Si* represents the injected node power, *V*i represents relevant node voltage, *Ii*, *Si* and *V*i are all 3X1 matrixes in the three-phase power distribution network, and the elements of the matrixes are complex numbers, "*" means the conjugation of the complex numbers, *I*ij represents the branch current matrix and is also a 3X1 matrix, the head and tail nodes of a branch are respectively identified as *i* and *j*, C represents the set of all nodes (except node *i*) connected to node *j*, *Z*ij represents the branch impedance matrix with the order of 3X3.

Equality constraints can be met during the model calculation process, but the inequality constraints can be integrated to the objective function through the constraint penalty, and the specific representation is as follows:

$$\begin{cases} F(X_i) = f(X_i) + k_f \sum_{j=1}^{N_{ueq}} \left(\max\left[0, -g_j(X_i)\right] \right) \\ g_j(X_i) < 0,\ j = 1, 2, \cdots, N_{ueq} \end{cases} \quad (4)$$

Where *F(Xi)* is the objective function for state estimation integration, N_{ueq} is the quantity of the inequality constraints mentioned in Formula (2), *gi(Xi)* is the inequality constraints set of Formula (2), *kf* is the penalty factor and is set as 1000 in the experimental research.

2.3. State measurement Configuration of the Power Distribution Network

The state measurement of the three-phase power distribution network mainly includes pseudo measurement and real-time measurement, and the state measurement configuration adopted in this paper is as shown in Figure 1.

Real-time measured states include:

(1) For RTU (Remote Terminal Unit): active and reactive power, voltage and current amplitude.

(2) For outgoing switches of the transformer substation (S/S): active and reactive power, voltage and current amplitude.

Pseudo measured states include:

(1) For determined load: active and reactive power, voltage and current amplitude; for uncertain load: voltage amplitude, mean active power and change amplitude, power factor.

(2) For determined DG (Distributed Generator): active and reactive power, voltage amplitude; for uncertain DG: voltage amplitude, mean active power and change amplitude, power factor.

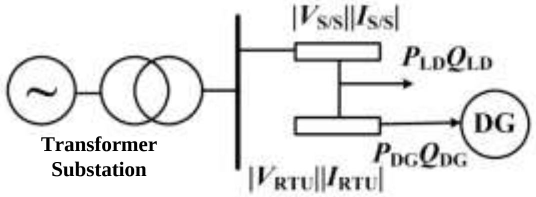

Figure 1. Hardware Configuration for Measurement

3. Multi-agent Collaborative IWD State Estimation

3.1. IWD Algorithm

IWD algorithm implementation parameters include: water drop velocity *velocity*(*IWD*) and river-way soil content *soi*l(*IWD*), wherein parameters *velocity*(*IWD*) and *soi*l(*IWD*) are continuously updated during algorithm evolution. Specifically, the water drop updates and searches soil content in the aside area in order to continuously find the shortest path and accordingly find the optimal path to the target position, as shown in Figure 2.

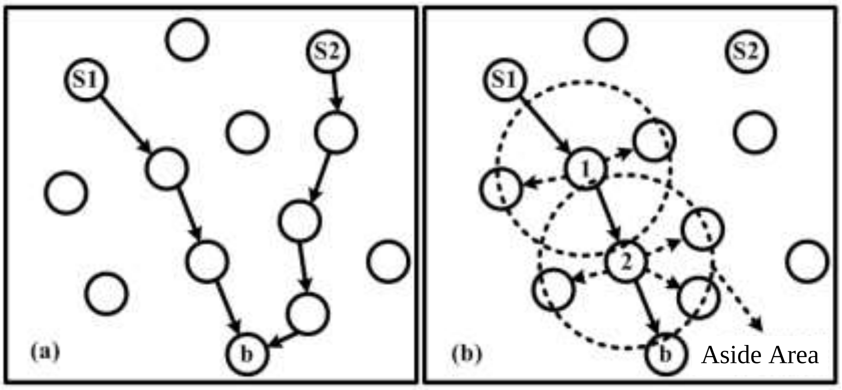

Figure 2. Intelligent Water Drop Path Update

During the movement of the intelligent water drop from river-way position *i* to river-way position *j*, the velocity variation of the water drop is $\Delta velocity(IWD)$, and this water drop parameter variation is nonlinearly inversely proportional to the soil content $soil(i,j)$ from river-way position *i* to river-way position *j*.

$$\Delta velocity(IWD) = \frac{a_v}{b_v + c_v\left(soil(i,j)\right)^2} \tag{5}$$

In Formula (5), parameters *av*, *bv* and *cv* are the parameters preset according to the specific problems. During the flowing process of the water drop, the river-way soil content is consistent with the variation of the soil carried in the water drop:

$$\Delta soil(IWD) = \Delta soil(i,j) \tag{6}$$

Since river-way soil content $soil(i,j)$ can inhibit the movement of the water drop, with the speed influence value as $\Delta velocity(IWD)$, the river-way soil content variation is nonlinearly inversely proportional to time *time(i, j)* for the movement of the water drop from river-way position *i* to river-way position *j*.

$$\Delta soil(IWD) = \frac{a_s}{b_s + c_s\left(time(i,j)\right)^2} \tag{7}$$

In Formula (7), parameters *av*, *bv* and *cv* are defined as the same as the parameters in Formula (5). Movement time parameter *time(i, j)* can be calculated according to the physical calculation formula regarding speed and distance.

$$time(i,j) \propto \frac{d(i,j)}{velocity(IWD)} \tag{8}$$

In specific IWD algorithm implementation, the time parameter for the movement of the water drop from river-way position *i* to river-way position *j* is calculated as follows:

$$time(i,j) = \frac{HUD(i,j)}{velocity(IWD)} \tag{9}$$

In Formula (9), parameter *HUD(i, j)* is the reverse heuristic function, and the rest soil content of the river-way passed by the water drop is calculated as follows:

$$soil(i,j) = \rho_0 \times soil(i,j) - \rho_n \times \Delta soil(i,j) \tag{10}$$

In Formula (10), parameters ρ_0 and ρ_n are the weight parameters of the heuristic function and can meet the following conditions:

$$\rho_0 + \rho_n = 1 \tag{11}$$

After the movement of the water drop and the soil exchange with the river-way soil, the soil content of the water drop is updated as follows:

$$soil(IWD) = soil(IWD) + \Delta soil(i,j) \tag{12}$$

River-way soils can impede the movement of the water drop, so the water drop may have a large probability of flowing along the path with small obstruction (small soil content), namely with large flow rate. Such probability $p(i, j)$ can be defined as follows:

$$\begin{cases} p(i,j) = \dfrac{f\left(soil(i,j)\right)}{\sum_k f\left(soil(i,j)\right)} \\ f\left(soil(i,j)\right) = \dfrac{1}{\varepsilon + g\left(soil(i,j)\right)} \end{cases} \tag{13}$$

In Formula (13), ε is a constant value (positive value); g is adopted to ensure that the river-way soil content variation is a positive value and is calculated as follows:

$$g\left(soil(i,j)\right) = \begin{cases} soil(i,j), if \ \min\left(soil(i,j)\right) > 0 \\ soil(i,j) - \min\left(soil(i,j)\right), else \end{cases} \tag{14}$$

In Formula (14), min(*soil*(*i, j*)) is the minimum soil content along the way from river-way position *i* to river-way position *j*.

3.2. Multi-agent Algorithm Structure

The multi-agent intelligent water drop algorithm structure includes two kinds of water drop clusters: first, the management agent is responsible for the main water drop cluster; second, the sub-agent is responsible for managing the water drop sub-cluster. Specifically, the main water drop cluster is responsible for controlling the loop iteration process for water drop evolution, and the co-evolution of the water drop sub-cluster and the main water drop cluster is realized through information interaction, and the process is as follows:

Step 1: (Optimal Value Sharing) The main water drop cluster can search the feasible solutions through iteration, and then share the global optimal solution *gbest* to the water drop sub-clusters after the expiry of the interaction period;

Step 2: (Search of Dimensionality 1) Water drop sub-cluster 1 obtains *gbest* through information interaction and takes it as the initial value to search dimensionality 1 of the state variable, and sends the result to the position of dimensionality 1 of *gbest* after the search process is ended;

Step 3: (Search of Dimensionality 2) The main water drop shares the updated *gbest* to water drop sub-cluster 2, and then water drop sub-cluster 2 takes *gbest* as the initial value to search dimensionality 2 of the state variable, and sends the result to the position of dimensionality 2 of *gbest* after the search process is ended;

Step 4: (Search of All Dimensionalities) Similarly, all sub-clusters of *gbest* are updated, and the solution is transmitted to the main water drop cluster.

Step 5: (Convergence Judgment) The main water drop cluster executes the collaborative search in *Ns*-dimensional space to obtain new *gbest* and meanwhile judge whether this optimal value can meet the convergence conditions: if yes, terminate the algorithm; if no, return to Step 1.

3.3. Flow Chart of the Algorithm

The flow chart of the proposed algorithm is as shown in Figure 3.

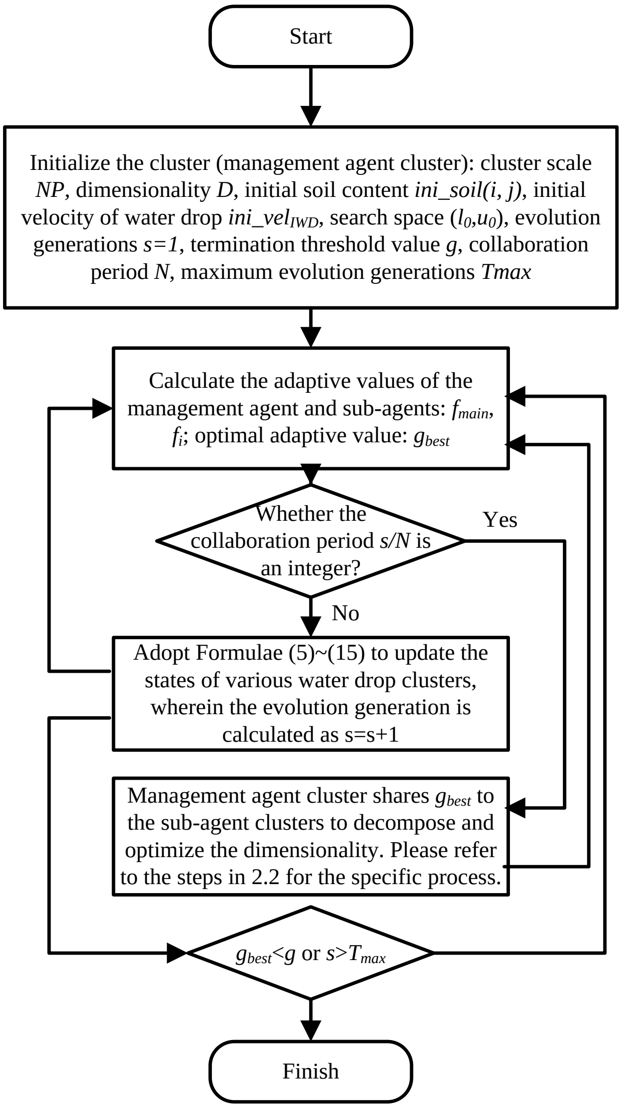

Figure 3. The Flow Chart of the Intelligent Water Drop Algorithm

In the algorithm flow as shown in Figure 3, the initialization parameters of the algorithm include cluster scale *NP*, dimensionality *D*, initial soil content *ini_soil(i, j)*, initial velocity of water drop *ini_velIWD*, search space (*l0*,*u0*), evolution generations *s=1*, termination threshold value *g*, collaboration period *N*, maximum evolution generations *Tmax*. Generally, the initial state of the water drop is updated as follows:

$$\begin{cases} \mathbf{X} = \left[\mathbf{X}_1, \mathbf{X}_2, \cdots, \mathbf{X}_{N_s}\right] \\ x_m = rand \times \left(P_{\mathrm{DG,max}}^m - P_{\mathrm{DG,min}}^m\right) + P_{\mathrm{DG,min}}^m \\ x_n = rand \times \left(P_{\mathrm{LD,max}}^n - P_{\mathrm{LD,min}}^n\right) + P_{\mathrm{LD,min}}^n \end{cases} \tag{15}$$

Where Xi=[*xi*]*1xn*, *j*=1,2,…,*Ns*, *xj* is the state variable, *m*=1,2,…,*Ng*, *n*= *Ng* +1, *Ng*+2,…, *Ng*+ *NL*, *rand* is the random function, *Ns* is the state quantity, *NL* is the quantity of the loads to be estimated, and *Ng* is the quantity of the distributed generators to be estimated.

4. Example Analysis

Matlab simulation platform is adopted for the experimental analysis, IEEE 57-bus standard calculation examples are selected as the simulation calculation examples, and the distributed generators are set in the above power distribution network calculation examples. Relevant parameters of the multi-agent intelligent water drop algorithm are set as follows: the number of the management agent (main water drop) clusters is set as 80, the scale of the sub-agent cluster (water drop sub-clusters) is selected as 30, the maximum cluster iteration is set as 1000, and the collaboration period is set as N=45. Please refer to Literature [12] for the parameter setting of the intelligent water drop algorithm.

4.1. Generator and Uncertain Load State Estimation

IEEE 57-bus network system is as shown in Figure 4, and this system includes four distributed generators and 6 uncertain loads, wherein the power, the position and the deviation of the distributed generators are as shown in Table 1, and relevant data information of the uncertain loads is as shown in Table 2. The nominal voltage of IEEE 57-bus system is 4.17kV, and the positions for real-time voltage measurement are nodes 21, 36, 43 and 52, and the voltage simulation value thereof is obtained through adding Gaussian deviation to the flow calculation value, wherein Gaussian distribution is N(0, 0.0012).

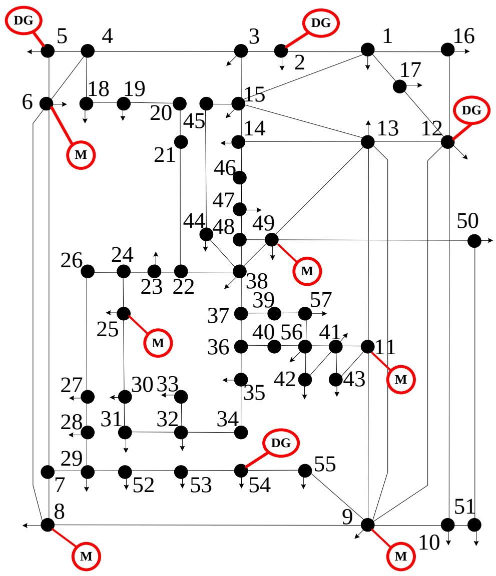

Figure 4. IEEE 57-bus Network System

Table 1. Distribution Generator Information of 57-bus IEEE System

Node	Type	Voltage Deviation/%	Active Power/kW	Active Deviation/%	Power Factor
2	Photovoltaic Generator	1.1	[100,0,0]	16	0.96
5	Wind Generator	1.2	[0,100,0]	16	0.96
12	Photovoltaic Generator	1.1	[150,150,150]	16	0.96
54	Wind Generator	1.2	[150,150,150]	16	0.96

Table 2. Uncertain load information

Node	Voltage Deviation/%	Active Power/kW	Active Deviation/%	Power Factor
7	1.1	[0,0,20]	15	[~,~,0.87]
9	1.1	[40,0,0]	20	[0.87,~,~]
12	1.1	[0,20,0]	25	[0.81,0.81,0.81]
19	1.1	[35,35,35]	30	[0.81,0.81,0.81]
24	1.1	[35,35,70]	25	[~,0.87,~]
48	1.1	[105,70,70]	20	[0.87,~,~]

The state estimation realized by the proposed dimensionality-decomposed intelligent water drop for IEEE 57-bus, uncertain load and distributed generator is as shown in Table 3.

Table 3. Distributed Generator and Load State Estimation

Node	Active Power/kW	
	Actual Value	Estimated Value
2	[100,0,0]	[99.8,0,0]
5	[0,100,0]	[0,99.9,0]
12	[150,150,150]	[150.1,149.8,149.9]
54	[150,150,150]	[149.5,149.8,150.1]
6	[0,0,20]	[0,0,19.9]
8	[40,0,0]	[39.7,0,0]
10	[0,20,0]	[0,20.1,0]
11	[35,35,35]	[35.1,35.2,34.8]
25	[35,35,70]	[35.1,34.9,70.2]
49	[105,70,70]	[105.4,69.6,70.3]

The power factors of the distributed generators and uncertain loads are give in Tables 1~2, so there is no need to estimate the reactive power. According to the simulation results shown in Table 3, the estimated values calculated by the dimensionality-decomposed intelligent water drop algorithm for IEEE 57-bus system state is very approximate to the actual value.

4.2. State estimation Error Comparison

In order to further numerically evaluate the algorithm performance, two evaluation indexes are defined: (1) MIAE (Maximum Absolute Error); (2) MIRE (Maximum Relative Error). The definitions are as follows:

$$E_{MIRE}(\%) = \max\left(\frac{\left|X_{est}(i) - X_{true}(i)\right|}{X_{true}(i)}\right) \times 100 \tag{16}$$

$$E_{MIAE}(\%) = \max\left(\left|X_{est}(i) - X_{true}(i)\right|\right) \tag{17}$$

IWD algorithm, SA-PSO (Simulated Annealing Particle Swarm Optimization) algorithm and CO-ACO (Collaborative Ant Colony Optimization) algorithm are selected as the comparison algorithms, and the estimation error comparison is as shown in Table 4, and the algorithm convergence is as shown in Figure 6.

Table 4. Estimation Error Comparison

Distributed Generator Estimation Error				
Algorithm	MIRE		MIAE	
	MIRE Error Value (%)	Node Position	MIAE Error Value (%)	Node Position
IWD	9.16/9.16/9.16	2/5/2	9.75/9.71/9.89	2/5/2
SA-PSO	3.27/3.49/3.53	5/5/12	5.68/5.24/5.51	5/5/12
CO-ACO	2.74/2.62/2.83	5/2/2	3.82/3.64/3.53	5/2/2
MAIWD	0.71/0.71/0.71	5/5/5	0.82/0.82/0.82	5/5/5
Uncertain Load Estimation Error				
Algorithm	MIRE		MIAE	
	MIRE Error Value (%)	Node Position	MIAE Error Value (%)	Node Position
IWD	8.63/6.92/7.58	21/28/47	9.93/9.84/9.86	41/28/47
SA-PSO	3.87/4.26/4.97	47/47/59	4.37/4.95/5.16	32/45/59
CO-ACO	3.13/2.95/4.38	47/34/47	4.27/4.32/4.46	38/42/51
MAIWD	0.83/0.77/0.93	24/47/47	0.93/0.98/0.95	47/47/47

In Table 4, the three-phase maximum error values of different algorithms are shown in “Error Value” column, and the node positions of the maximum estimation errors are shown in “Node Position” column. The measured values are different from each other, so the above maximum absolute errors and maximum relative errors appear at different nodes. According to the data in Table 4, the maximum relative error of MAIWD algorithm for the distributed generators is 0.71%, significantly lower than the error value shown in Table 1. The maximum relative error of MAIWD algorithm for the loads is 0.93%, significantly lower than the error value shown in Table 2. Compared with IWD, SA-PSO and CO-ACO algorithms, MAIWD algorithm has lower estimation error. According to the object convergence comparison curve shown in Figure 5, the proposed MAIWD algorithm is superior to the comparison algorithms in the aspects of convergence speed and accuracy.

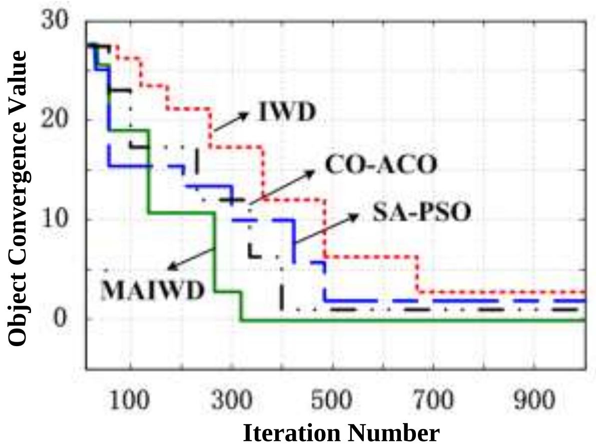

Figure 5. Objective Function Convergence Curve

4.3. Comparison under Different Network Scales

The standard calculation examples of four differently scaled networks, namely IEEE 13-bus, IEEE 37-bus, IEEE 57-bus and IEEE 123-bus, are selected for the experimental comparison. The simulation results are as shown in Figure 6.

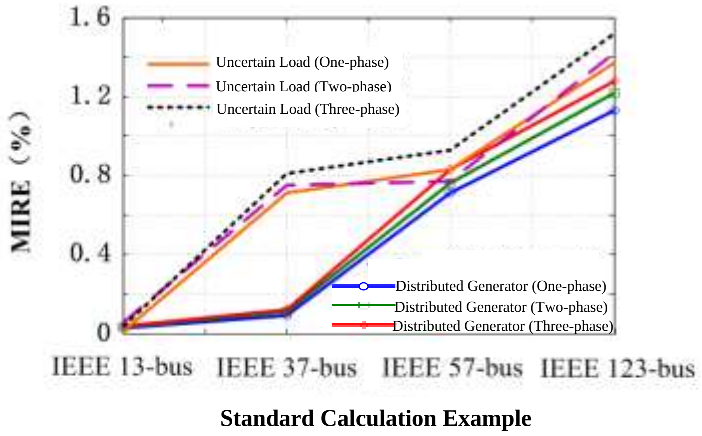

(a) MIRE Index comparison

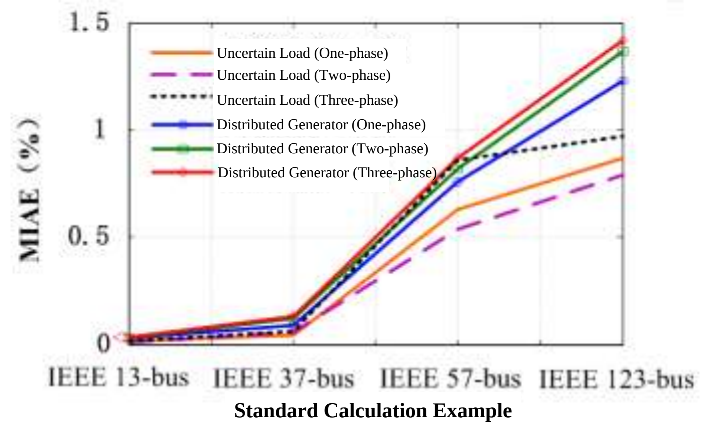

(b) MIAE Index comparison

Figure 6. Comparison of Different System State Estimation Errors ((a) MIRE Index Contrast; (b) MIAE Index Contrast)

Figures 6a and 6b respectively show the estimation errors of MAIWD algorithm for the calculation examples in the above four standard power distribution networks. According to the simulation figures, the estimation errors of the algorithm for the distributed generators and the uncertain loads are increased along with the increase of the system complexity, and this is consistent with the objective practice.

5. Conclusion

The state estimation fitting function with constraints integrated items is designed in this paper to realize the unconstrained operation of the algorithm. Meanwhile, the multi-agent co-evolution method is adopted to improve IWD algorithm, and sub-agent evolution results are constantly introduced therein to update the dimensionality of the global optimal solution, thus to realize the collaborative balanced decomposition of the high-dimensional optimization problem. Relevant experiment is carried out to not only compare the advantages of the proposed algorithm in the aspects of state estimation accuracy and speed, but also show the comparison results of different algorithms and the estimation errors of the standard calculation examples with different complexities. The above MAIWD algorithm has good dimensionality decomposition effect for the calculation examples with high complexity, but due to the complex algorithm design thought, the robustness of the algorithm for implementation and practical application should be further verified.

References

[1] C. Fu, P. Zhang and J. Jiang, “A Bayesian approach for sleep and wake classification based on dynamic time warping method”, Multimedia Tools and Applications, **(2015)**, pp. 1-20.
[2] Z. Lv, “Wearable smartphone: Wearable hybrid framework for hand and foot gesture interaction on smartphone”, Computer Vision Workshops (ICCVW), IEEE International Conference, IEEE, (2013).
[3] Y. Lin, J. Yang and Z. Lv, “A Self-Assessment Stereo Capture Model Applicable to the Internet of Things”, Sensors, vol. 15, no. 8, (2015), pp. 20925-20944.
[4] J. Yang, S. He and Y. Lin, “Multimedia cloud transmission and storage system based on internet of things”, Multimedia Tools and Applications, (2015), pp. 1-16.
[5] Z. Lv, T. Yin and Y. Han, “WebVR——web virtual reality engine based on P2P network”, Journal of Networks, vol. 6, no. 7, (2011), pp. 990-998.
[6] Z. Lv, A. Tek and F. Da Silva, “Game on, science-how video game technology may help biologists tackle visualization challenges”, PloS one, vol. 8, no. 3, (2013), pp. 57990.
[7] T. Su, W. Wang and Z. Lv, “Rapid Delaunay triangulation for randomly distributed point cloud data using adaptive Hilbert curve”, Computers & Graphics, vol. 54, (2016), pp. 65-74.
[8] J.-Y. Hu, Z.-W. Gao and W.-S. Pan, “Multiangle Social Network Recommendation Algorithms and Similarity Network Evaluation”, Journal of Applied Mathematics, (2013).
[9] S. Zhou, L. Mi, H. Chen and Y.-S. Geng, “Building detection in Digital surface model”, IEEE International Conference on Imaging Systems and Techniques (IST), (2012).
[10] J. He, Y.-S. Geng and K. Pahlavan, “Toward Accurate Human Tracking: Modeling Time-of-Arrival for Wireless Wearable Sensors in Multipath Environment”, IEEE Sensor Journal, vol. 14, no. 11, (2014), pp. 3996-4006.
[11] Z. Lv, A. Halawani and S. Fen, “Touch-less Interactive Augmented Reality Game on Vision Based Wearable Device”, Personal and Ubiquitous Computing, vol. 19, no. 3, (2015**)**, pp. 551-567.
[12] G.-Q. Bao, L. Mi, Y.-S. Geng, M.-D. Zhou and K. Pahlavan, “A video-based speed estimation technique for localizing the wireless capsule endoscope inside gastrointestinal tract”, 36th Annual International Conference of the IEEE Engineering in Medicine and Biology Society (EMBC), **(2014)**.
[13] D.-G. Zeng and Y.-S. Geng, “Content distribution mechanism in mobile P2P network”, Journal of Networks, vol. 9, no. 5, **(2014)**, pp. 1229-1236.

Author

Li Shuqiang, He received his Ph.D. in agricultural engineering from China Agricultural University in Beijing, China. He is currently a lecturer in the Henan University of Science and Technology in Luoyang, China. His research interest is mainly in the area of Precision Agricultural, Agricultural Engineering. He has published several research papers in scholarly journals in the above research areas and has participated in several books.